

# Power coordination in a fuel cell–battery hybrid power source using commercial power controller circuits

M.J. Blackwelder, R.A. Dougal\*

*Department of Electrical Engineering, University of South Carolina, Columbia, SC 29208, USA*

Received 2 February 2004; accepted 27 February 2004

Available online 2 Jun 2004

## Abstract

Hybrid power systems combine the superb energy density of a fuel cell power source with the outstanding power density of modern batteries. A hybrid power source with an integral power distribution and charge management system was designed and built using standard miniature power regulator integrated circuits with appropriate modifications to implement the necessary controls. The resulting converter not only allows the interconnection of fuel cell systems and batteries having dissimilar operating voltages, but it also imposes a power sharing strategy that elicits peak performance from each part of the device. The resulting hybrid power source can supply 70% greater peak power, with only a 6% increase in weight, and no increase in volume, compared to the as-packaged fuel cell power source on which the hybrid source was based.

© 2004 Elsevier B.V. All rights reserved.

*Keywords:* Fuel cell; Battery; Hybrid; System control; Power conversion; Portable power source

## 1. Introduction

Since Sir William Grove discovered the basic hydrogen–oxygen fuel cell in 1839, great strides have been made in fuel cell technology. The proton exchange, or polymer electrolyte membrane (PEM), fuel cell verges on becoming a viable power source.

Although the energy density of PEM fuel cells is excellent, the specific power and power density are low compared with many types of batteries. To come closer to achieving both the energy density of fuel cells and the power density of batteries, the two devices can be combined to form hybrid power sources, as shown in Fig. 1.

The concept of hybridization is currently used in some conventional automobiles to increase the peak power available for acceleration, while the internal combustion engine operates at optimal efficiency [1]. Hybridization also allows recapture of kinetic energy when braking. This same concept of power leveling has been studied for fuel cell powered vehicles, such as submarines [2], automobiles [3,4], golf carts [5] and scooters [6]. The hybrid concept is also advantageous in small scale, low power and portable fuel cell power sources [7–12].

Hybrid power sources can be classified as either “active” or “passive” depending on whether or not active electronic circuits are used to manage power flow between the elements within the source. In this paper we will first describe the functional characteristics of passive hybrid power sources, especially focusing on the shortcomings of the passive approach, and then we will describe an active hybrid that overcomes these disadvantages.

### 1.1. Background

Fig. 2 shows the topology of a passively connected hybrid power source [2,12]. In this topology the fuel cell and battery are directly connected to the load so, obviously, the terminal voltages of the battery and the fuel cell must be similar and compatible. Fig. 3 presents the voltage versus current characteristics of the fuel cell and the battery in this system when the battery is fully charged. If the battery and fuel cell have similar power ratings, then they will also have similar equivalent series resistances, hence the slopes of the  $V-I$  curves will be similar.

One can see from Fig. 3 that the initially sharp drop in fuel cell voltage at low currents (caused by the activation overpotential) will cause the battery discharge current to be always larger than the fuel cell current, even at low power demand where the fuel cell could otherwise by itself supply all the

\* Corresponding author. Tel.: +1-803-777-7890; fax: +1-803-777-8045.  
E-mail address: [dougal@engr.sc.edu](mailto:dougal@engr.sc.edu) (R.A. Dougal).

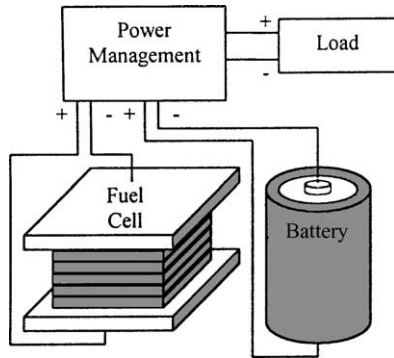


Fig. 1. Parallel hybrid power source.

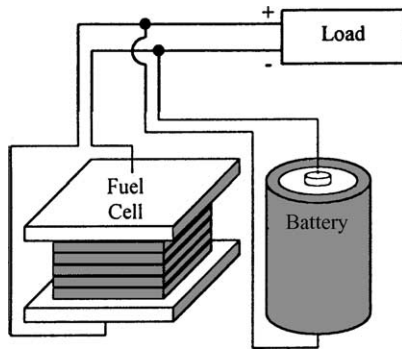


Fig. 2. Passively connected fuel cell and battery hybrid.

load power demand. In this situation, eventually the battery must become at least partially depleted. Thus this form of passive hybrid cannot fully utilize the power capabilities of the fuel cell before drawing power from the battery.

Fig. 4 shows the voltage versus current characteristics of the same components after the battery becomes partially depleted. The battery can be charged only at those very low currents where the fuel cell voltage exceeds the battery voltage. In this case, it is not possible to recharge the battery until there is very little power demand from the load. Although the fuel cell operates very efficiently at high terminal voltages, corresponding to low currents, the power that is available to charge the battery at that high voltage is only

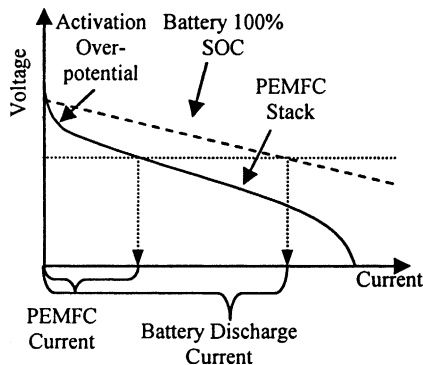


Fig. 3. Voltage–current characteristics of a fuel cell and a fully charged battery.

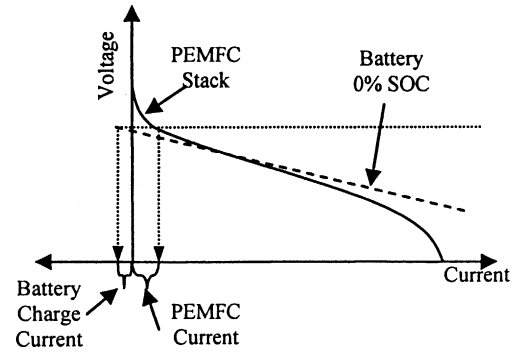


Fig. 4. Voltage and current characteristics of fuel cell and battery, with battery partially depleted.

a small fraction of the inherent power capability of the fuel cell.

As the ratio of peak load power to average load power increases, the power sharing and recharging issues are exacerbated. This is because the battery will be designed to supply the peak power and the fuel cell will be designed to supply the average power. As the power rating of the battery becomes greater compared to that of the fuel cell, the equivalent series resistance will become less and the slope of the battery curve shown in Figs. 3 and 4 will flatten.

Some of these problems can be alleviated by moving to a simple active hybrid configuration such as that described by Han and Park [10] which employs a voltage limiter to clip the highest fuel cell voltages (at low currents) to prevent overcharging the battery.

Fig. 5 presents the topology of such a simple active fuel cell and battery hybrid power source. As can be seen in Fig. 6, voltage limiting allows the fuel cell to provide a larger fraction of power to the load, compared to the passive hybrid, at any value of load power demand. This is an improvement over the passive connection, but still the fuel cell cannot operate at its maximum power point without at least partially depleting the battery.

Fig. 7 shows the characteristics of the same components when the battery is fully depleted. The fuel cell can now supply more power to the battery, at the same load voltage, than it did with a passive connection. Although this is an

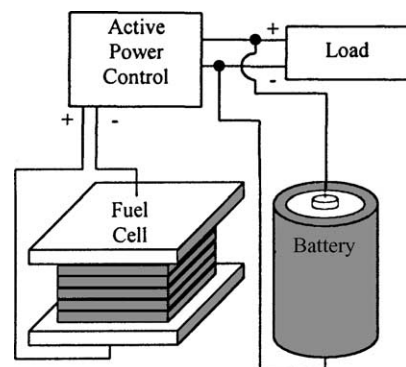


Fig. 5. Actively connected fuel cell and battery hybrid.

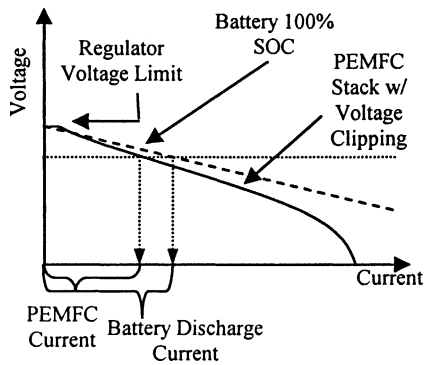


Fig. 6. Voltage vs. current characteristics of fuel cell with voltage clipping and fully charged battery.

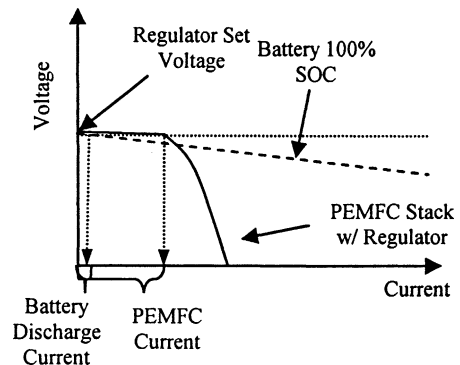


Fig. 8. Voltage vs. current characteristic of fuel cell with voltage regulator and fully charged battery.

improvement over the passive connection, still the fuel cell may not be capable of recharging the battery at the maximum power that the fuel cell *could* produce. Again, this is due to the fact that the fuel cell and battery have similar power ratings, yet only a small fraction of the fuel cell power is available to recharge the battery, and the fraction decreases as the battery state of charge increases.

Nadal and Barbir [3] improved on this design by choosing the system design parameters so that the voltage of the fuel cell at its maximum power point was equal to the voltage of the fully charged battery. The voltage limiter was then set at that same voltage. The operating characteristics for this “regulated” active hybrid are shown in Fig. 8.

Unlike the previous systems, in this regulated system the fuel cell provides 100% of the load power until the power source voltage drops below the regulation voltage. Beyond this point, the battery supplies any amount of the load power that exceeds the capability of the fuel cell. Unfortunately, beyond this point, the ability of the fuel cell to supply power begins to decrease since the voltage is below the voltage corresponding to the maximum power point of the fuel cell. The battery becomes doubly taxed; it must provide all the load power beyond the maximum power capability of the fuel cell, plus the difference between the maximum power capability of the fuel cell and the smaller power that it can actually produce at the lower terminal voltage.

Fig. 9 shows the operational characteristics of the same regulated active hybrid with a depleted battery. Notice that the battery can be recharged at close to the maximum power available from the fuel cell.

This is a dramatic improvement over the two previous methods, which used only a small fraction of the maximum power available from the fuel cell. Yet, for some combinations of battery chemistry and capacity, the maximum power available from the fuel cell may exceed the maximum power that the battery can accept during recharging. This can be a problem under no-load conditions.

Nadal and Barbir [3] resolved this problem by dynamically adjusting the regulator voltage set point to limit the recharge rate of the battery. This is less of a problem as the ratio of peak to average power increases, which tends to decrease the power rating of the fuel cell compared to the battery and naturally limits the recharge rate.

Considering the disadvantages of the passive or the simple active hybrid power source configurations, we set out to design a more complex but more efficient and effective hybrid power source based on conventional power conversion control circuitry. Our work fully addresses all the adverse properties of the hybrid power sources previously described.

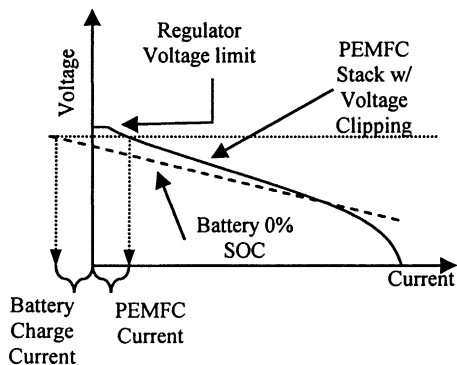


Fig. 7. Voltage vs. current characteristics of fuel cell with voltage clipping and partially depleted battery.

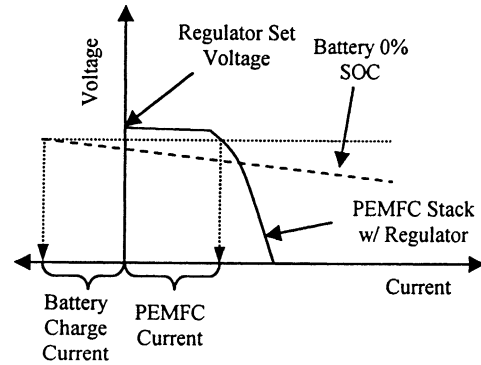


Fig. 9. Voltage vs. current characteristic of regulated fuel cell and battery with partially depleted battery.

## 2. Design

### 2.1. Active hybrid power source

We designed to achieve a low cost system using generic off-the-shelf power management components. This design will not only safely manage power flow in a lithium ion (Li-ion) battery, but also it will draw maximum power from the fuel cell system before tapping the battery to meet any higher power needs. A high-level schematic illustration of the system is shown in Fig. 10.

#### 2.1.1. Power controller

Power control is based on the peak current mode strategy commonly used for DC/DC power converters. Two commercially available power integrated circuits were used to build the power controller; an LTC<sup>®</sup>1435IS high efficiency, low noise, synchronous, step-down switching regulator and an LTC<sup>®</sup>1621IGN rail-to-rail current sense amplifier.

The conventional structure of a peak current mode regulator is shown in black in Fig. 10. There are two control loops, one nested within the other. The inner, high-bandwidth control loop forces the average switch current to track an average current reference signal. This loop has a ceiling to protect the solid-state switches from excessive currents. The second, outer loop uses the LTC<sup>®</sup>1435IS proportional-integral error amplifier to adjust the average current reference so as to regulate the output voltage.

The poles of the voltage regulation control loop were placed so as to reduce oscillations. In conjunction with the large double layer capacitance of the battery itself, the pole placement produces a relatively long time constant

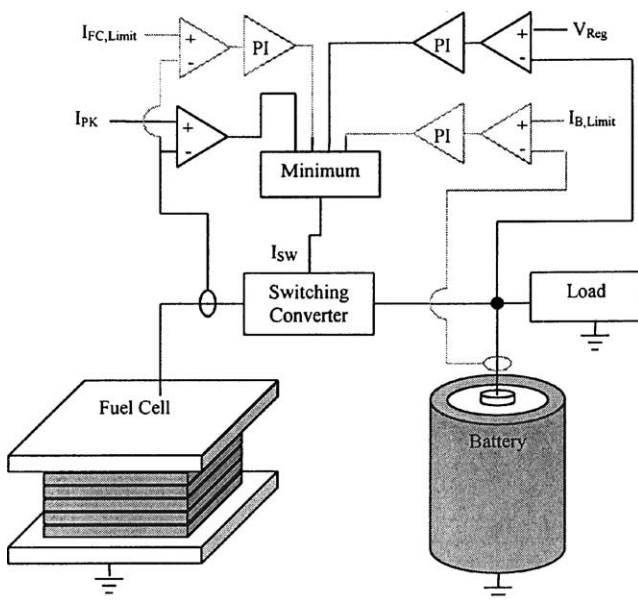


Fig. 10. Power control topology with standard peak current mode control (black) and added current and voltage control loops (gray).

which stabilizes the control circuit under high-speed load dynamics.

To achieve the further objectives of the hybrid power source two additional control loops were added as shown in gray in Fig. 10. The first loop limits the average current drawn from the fuel cell, independent of the terminal voltage, to a value no greater than that corresponding to the maximum power point. For terminal voltages below the regulation voltage this effectively makes the fuel cell operate as a fixed power source.

The second control loop limits the battery charging current by limiting the power output of the converter to the sum of the actual load demand plus the maximum safe battery charging power. Generally, this limit must be enforced only under low or no-load conditions and replicates the characteristics of any conventional lithium-ion battery charger that operates under the constant current–constant voltage (CC/CV) protocol [13].

This nonlinear control strategy allows any average current that hits its limit to dominate, whether it be the fuel cell current limit, the peak switch current limit, the battery charging current limit, or the voltage regulation current limit. Thus the converter operates in four different modes, changing modes as needed.

The power control hardware is pictured in Fig. 11. The electronic components are all surface-mount devices, so the size is dominated by the one power inductor, which itself could be reduced in size by using a powdered metal core rather than a ferrite core.

#### 2.1.2. Battery

The hybrid power source uses Sony US18650S hard carbon electrode lithium ion batteries. Four cells are connected in series to form a battery having a voltage at full charge of 16.8 V. Each cell has a 1.4 Ah (or  $\sim 5.0$  Wh) capacity.

To suit these batteries, the charging current and voltage limits of the control circuit were set to the battery manufacturers' suggested values of 1.0 A and 16.8 V.

Since Li-ion batteries must be operated within strict limits to prevent thermal run-away and the possibility of a fire or

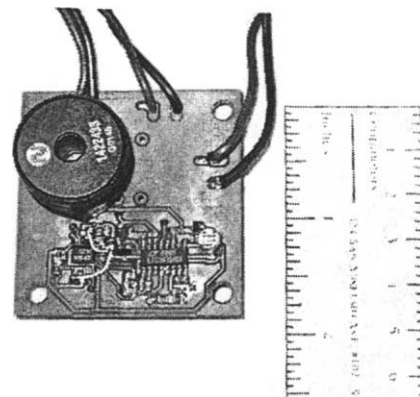


Fig. 11. Power controller.

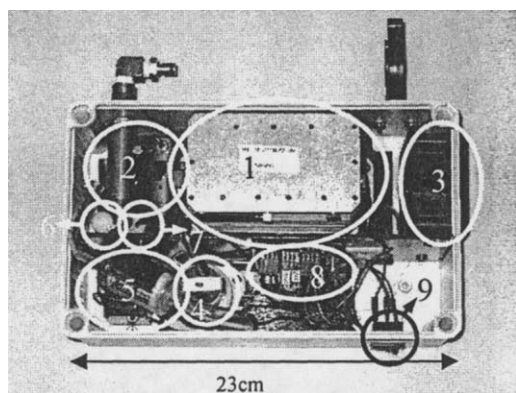


Fig. 12. H-Power D35 portable fuel cell power source.

explosion every consumer battery is assembled with some form of protection device, and some have an additional thermal current interruption device. The batteries used in these tests do not contain any solid-state protection circuits, but they do contain a thermally sensitive current interrupter. Although Li-ion batteries can be discharged at rates in excess of 3 C (with only small reduction of lifetime [14]) the thermal protection device limited our discharge rate in experiments to 1.5 C.

### 2.1.3. Fuel cell system

The PEM fuel cell used in this hybrid power source, pictured in Fig. 12, was a model D35 purchased from H-Power<sup>TM</sup>.<sup>1</sup> The fuel cell system consists of a 25-cell stack with an active area of 28.4 cm<sup>2</sup> (1), a two-stage, 20 kPa hydrogen regulating system (2), a cooling fan (3), an air pump (4) and charcoal/fiberglass filter (5), a hydrogen purge valve (6), a hydrogen inlet valve (7), a microcontroller (8), a voltage regulator (removed), a 9 V start-up battery (beneath 4) and an on-off switch (9). The nominal power capacity of the fuel cell system is 35 W at approximately 18.0 V. The entire system has a mass of 2.5 kg and a volume of 3360 cm<sup>3</sup>, not including fuel and fuel storage.

The D35 fuel cell stack is typically capable of producing 50–55 W. As designed, the fuel cell system consumes 15 W of the stack power to operate the cooling fan, air pump, hydrogen inlet valve, control electronics, hydrogen purge valve, and other auxiliary components. For this experiment, the air pump was powered externally so as to remove the system dynamics associated with this device. The cooling fan requires 2 W and is controlled by the manufacturer's original control board.

The manufacturer's voltage–current curve for the stack alone is shown in Fig. 13. In our control circuit the fuel cell current limit was set at 2.8 A so as to not overload the fuel cell system. The D35 system was fueled by a 10 l cylinder of compressed, high-purity hydrogen. The manufacturer's original 12 V regulator was replaced with our control circuitry.

<sup>1</sup> Purchased by Plug-Power<sup>TM</sup> who no longer supports the D35 product line.

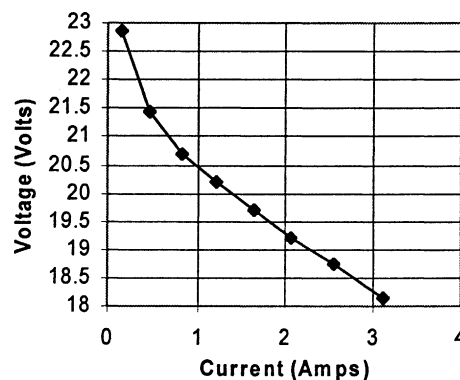


Fig. 13. Voltage–current characteristic of the fuel cell stack—from manufacturer's data.

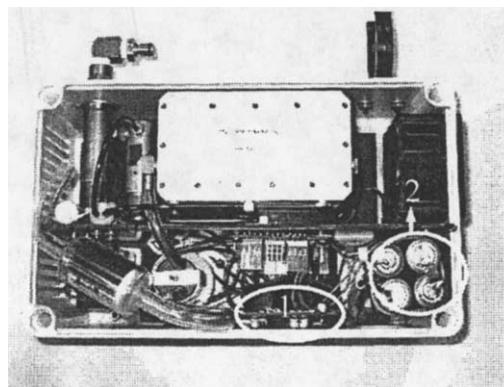


Fig. 14. Complete hybrid system.

The complete hybrid system, packaged in the original container, is shown in Fig. 14. The hybrid design allowed the original 9 V start-up battery and 12 V regulator to be removed. The resulting hybrid power source had the same volume as the original fuel cell system alone, and only 160 g more mass.

## 3. Experimental

### 3.1. Setup

A Chroma 63103 Programmable DC Electronic Load was used to draw power from the active hybrid power source. The electronic load was programmed to act as a power load (rather than as a current load or a resistive load) in order to replicate the behavior of most portable electronic devices that would normally be the loads on such a power source.

Fig. 15 shows a diagram of the experimental setup. The load voltage is the same as the battery terminal voltage since the load and battery are directly connected. The load current is the sum of the output current from the power controller and the battery current.

During all experiments, the battery and the power controller were positioned outside the D35 housing in order to conveniently fit test probes to the equipment.

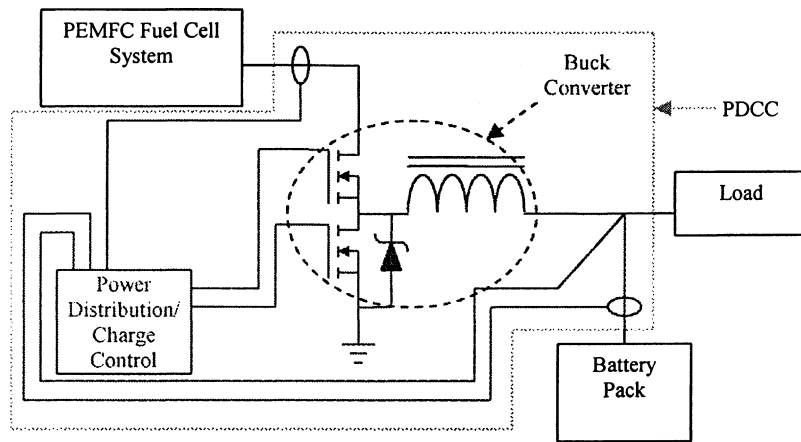


Fig. 15. Schematic illustration of the hybrid power source test system.

### 3.2. Verification of control objectives

The purpose of the first test was to verify that the fuel cell current limit was correctly enforced. A 70 W step load was applied to the hybrid power source. The resulting fuel cell stack current and voltage are shown in Fig. 16, which is a screen capture from the LeCroy LT374L oscilloscope that was used to record the system performance. The step load was applied at 2.5 ms. The current rose at a rate limited only by the inductance in the power converter. After 4 ms, the fuel cell current was limited to 2.8 A when the maximum fuel cell current limit control loop exerted control.

The high frequency hash visible in the fuel cell current results from the switching action of the power converter. The current pulses are easily absorbed by the double layer capacitance of the fuel cell, which eliminates any need for input filtering on the power converter. Unfortunately, these 200 kHz pulsed currents caused electro-magnetic interference (EMI) that coupled into the voltage measurements, as

observable in the fuel cell voltage waveform in Fig. 16. A more appropriate choice of power inductor core material and geometry would help to eliminate the EMI.

In the second test, we verified that the battery current limit was correctly enforced following a 70 W load dump at a time when the battery was partially depleted. The measured battery current and voltage are shown in Fig. 17. The load dump occurred at 5 ms. The battery current changed from 1.8 A discharging to approximately 1.0 A charging in just 0.5 ms, then stabilized within 4 ms.

The battery voltage limit was tested following a 70 W load dump with a fully charged battery. The results are shown in Fig. 18. The load dump occurred at 150 ms. The battery charging current limit immediately engaged to reduce the output current from the fuel cell to the battery safe maximum current. At 180 ms the voltage limit control loop began to override the charging current limit and reduced the charging current. The battery maximum voltage loop then adjusted the average current to obtain a stable 16.8 V at 450 ms.

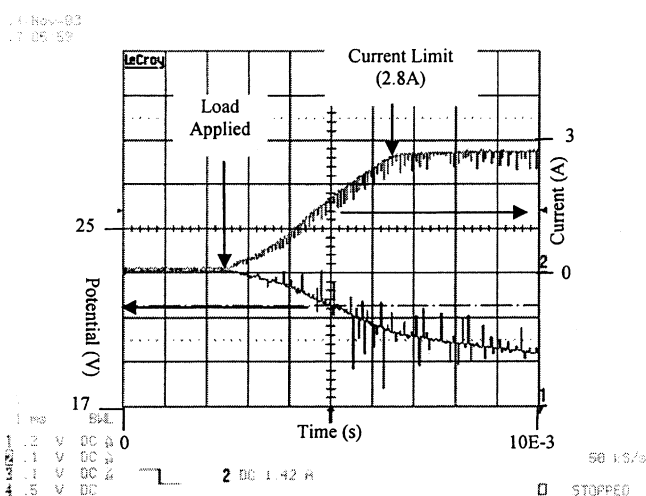


Fig. 16. Fuel cell current and voltage in test verifying engagement of the fuel cell maximum current limit mode.

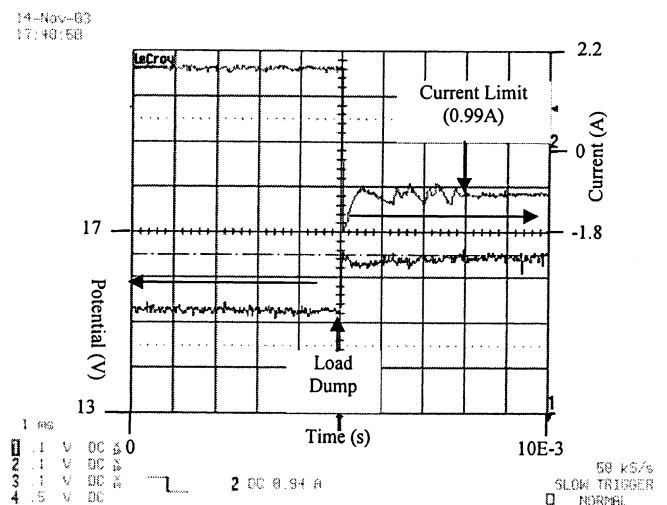


Fig. 17. Battery current and voltage in test verifying engagement of the battery maximum charging current limit mode.

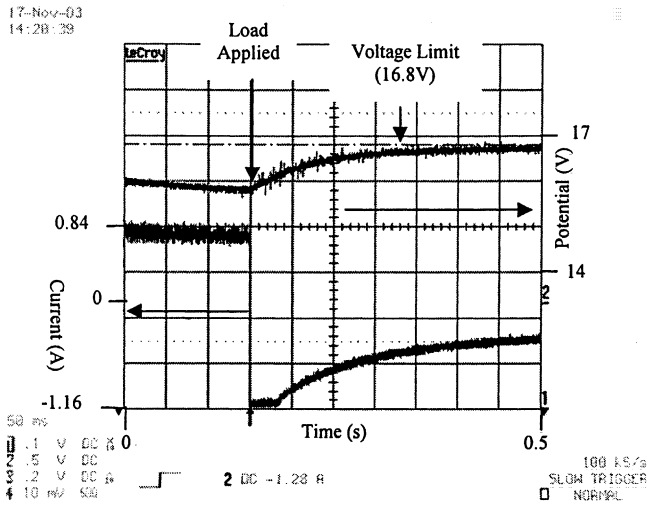


Fig. 18. Battery current and voltage during verification of engagement of charging voltage limit.

3.3. Load profile

The optimum proportioning of power and energy capacities between the battery and the fuel cell are highly application specific. In some cases, for example, for a load that requires very high peak to average power ratios and small volume, a highly power-dense storage device such as an electrochemical capacitor [15] may even be more desirable than a battery. In this test, we designed the load profile to maximally stress the particular hybrid source configuration that we had built.

The specific load profile we used is shown in Fig. 19. This profile uses most of the energy stored in the battery during the high-power phase and it allows the battery to recharge during the low-power phase while the fuel cell stack operates at close to its maximum power. This best displayed the full abilities of the hybrid power source. All the pertinent system data was recorded simultaneously during one load profile cycle.

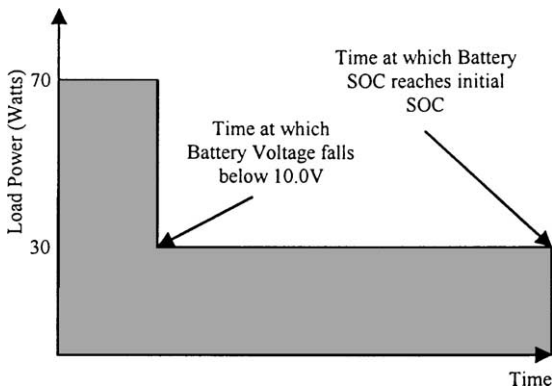


Fig. 19. Load profile for testing of hybrid power source.

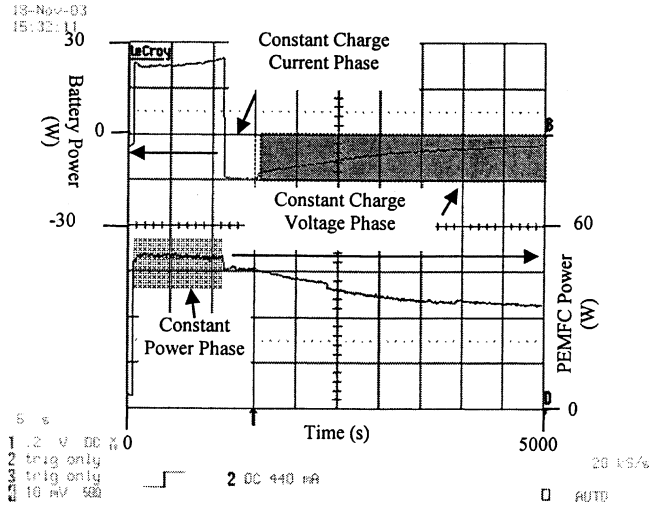


Fig. 20. Power produced by battery and PEMFC during load cycle.

4. Results

Fig. 20 shows the powers produced by the fuel cell and the battery during the load cycle shown in Fig. 19. During the high-power phase the fuel cell operated at its maximum power level and the additional load demand was met by the battery. The fuel cell continued to produce full power even as the battery was depleted and the terminal voltage of the power source dropped. At the onset of the low-power phase, the fuel cell continued to provide close to maximum power, which was then split between the load and the battery. As the battery became recharged and it reached the upper voltage limit the charging power reference decreased, and the sum of load and charging power tracked accordingly.

Fig. 21 shows the sum of the powers delivered by the fuel cell and the battery during the load cycle. During the high-power phase, the total power delivered by the hybrid

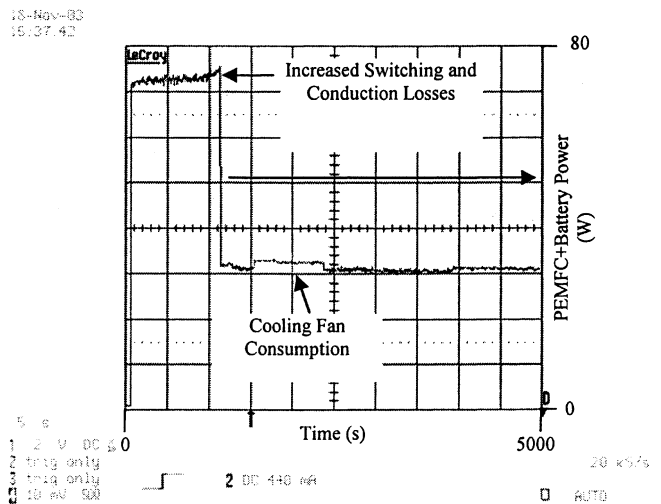


Fig. 21. Total power delivered by fuel cell and battery.

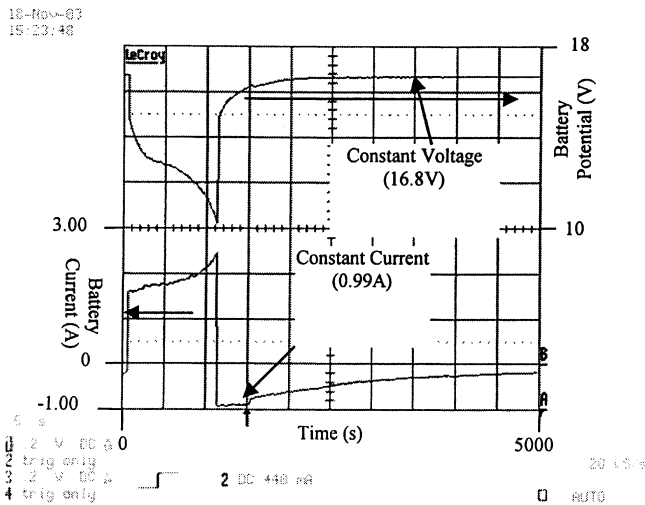


Fig. 22. Battery voltage and current.

source was 3 W greater than the power demanded by the load. This was the power lost in the power converter, which we then deduced to be 92% efficient. At the end of the high-power phase the total power delivered by the fuel cell and the battery increased slightly. This was due to the increase in load current as the battery voltage dropped. This increase in current increased the switching and conduction losses in the power converter.

At 1500 s the combined power delivered increased by 2 W for 800 s as the fuel cell stack cooling fan switched on. This did not reduce the load power or the battery charging power because the total power demand, including the power required by the fan, was less than the maximum power capacity of the fuel cell.

Fig. 22 shows the battery voltage and current. During the high-power phase, the battery provided power beyond the capability of the fuel cell. This continued until the battery voltage began to rapidly decline and therefore the battery current rapidly increased. This occurred at 1068 s. At this point the useful battery capacity was depleted and any load configured for a 4-cell Li-ion battery would have shut down due to low battery voltage. Initially charged to 80% capacity, the energy delivered by the battery up to this point was less than the initial state of charge.

The reasons that the battery did not provide full rated energy are threefold. First, at high discharge currents, the internal resistance of the battery caused the terminal voltage to drop below the safety cutoff voltage before the battery was fully discharged. The remaining energy *could* have been extracted at a lower power but not at the higher power level.

Secondly, at these high discharge rates, significant amounts of energy are dissipated inside the battery. In this case during the high-power phase an average of 1.8 A conducted through approximately 1.0 Ω of equivalent series resistance resulted in an average of 3.24 W converted from chemical energy to heat.

Table 1  
A continuously sustainable load profile

Power (W)	Duration (s)
70	1070
30	3930

Lastly, the battery was constructed from previously used cells which had slightly less capacity than new cells. This was done to measure the realistic performance of the hybrid power source.

During the low-power phase, the battery was recharged by the fuel cell as it simultaneously powered the load. The recharging dynamics followed the CC/CV protocol enforced by the controller. At the high-to-low load transition, the controller entered the battery current limit mode. The constant current phase ended at 1500 s, when the upper battery voltage limit was encountered. The constant voltage phase continued to 5000 s at which time the battery was recharging at 300 mA, which was identical to the initial condition under which the load cycle was started. Therefore, given sufficient fuel, the load profile of Table 1 can be continuously supported by this hybrid power source.

Fig. 23 shows the fuel cell voltage and current during the load cycle. During the high-power phase, the controller enforced the fuel cell current limit, thus fixing the fuel cell power production as shown in Fig. 20. There were slight transients in the fuel cell voltage that we believe were due to fluctuation in hydration and temperatures within the fuel cell stack.

During the low-power phase, the fuel cell voltage increased and the fuel cell current decreased, tracking the slowly reducing sum of charging power and load power. There was a slight dynamic at 2400 s when the cooling fan turned off.

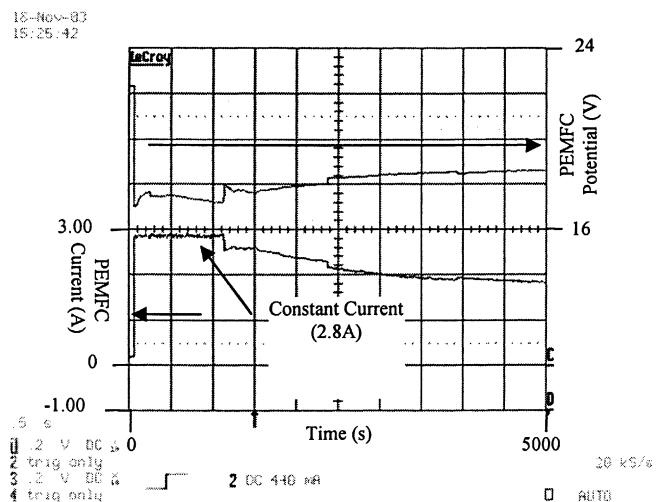


Fig. 23. Fuel cell voltage and current during load cycle.



## 5. Conclusions

A low cost (<\$ 22), light weight (<160 g), efficient (>90%), and compact (<32 cm<sup>3</sup>) solid-state power distribution and battery charge controller was designed and proven. The active power controller is extremely beneficial to operation of the hybrid power source. With no increase in volume and only a slight increase in mass (<6%) compared to the fuel cell alone, this hybrid power source offered many benefits compared to passive hybrids, including:

- One hundred percent of power is supplied by the fuel cell before any power is drawn from the batteries.
- The power converter offers the possibility to use fuel cell stacks and batteries having significantly different open circuit voltages.
- Batteries can be recharged at the maximum power capability of the fuel cell.

Further, compared to the voltage clamp hybrid configuration, the system described here provides:

- The fuel cell power is always limited to its safe maximum.
- The battery charging current is always limited to its safe maximum.

## Acknowledgements

This work was sponsored by the US Army Communications and Electronics Command under contract DAAB07-03-3-K416. Further support provided by the US Army RDECOM/CERDEC Fuel Cell Technology Team.

## References

- [1] G. Metrakos, et al., Strategy for increasing hybrid electric vehicle reversibility, Proc. Am. Contr. Conf. 1 (1997) 694–698.
- [2] J.C. Amphlett, et al., Dynamic interaction of a proton exchange membrane fuel cell and a lead-acid battery, J. Power Sources 65 (1997) 173–178.
- [3] M. Nadal, F. Barbir, Development of a hybrid fuel cell/battery powered electric vehicle, Int. J. Hydrogen Energy 21 (6) (1996) 497–505.
- [4] M. De Francesco, E. Arato, Start-up analysis for automotive PEM fuel cell systems, J. Power Sources 108 (2002) 41–52.
- [5] A. Funahashi, et al., Development of PAFC/battery hybrid system for golf cart, in: Proceedings of the 28th Intersociety Energy Conversion Engr. Conference, vol. 2, August 1993, pp. 217–222.
- [6] B. Lin, Conceptual design and modeling of a fuel cell scooter for urban Asia, J. Power Sources 86 (2000) 202–213.
- [7] T. Susai, et al., Development of a 1 kW polymer electrolyte fuel cell power source, J. Power Sources 92 (2001) 131–138.
- [8] J.W. Raadschelders, Energy sources for the future dismantled soldier, the total integration of the energy consumption within the soldier system, J. Power Sources 96 (2001) 160–166.
- [9] C.K. Dyer, Fuel cells for portable applications, J. Power Sources 106 (2002) 31–34.
- [10] J. Han, E.-S. Park, Direct methanol fuel-cell combined with a small back-up battery, J. Power Sources 112 (2002) 477–483.
- [11] P.B. Jones, et al., A hybrid power source for pulse power applications, J. Power Sources 80 (1999) 242–247.
- [12] L.P. Jarvis, Power assisted fuel cell, J. Power Sources 70 (1998) 253–257.
- [13] Li-Ion Rechargeable Battery Technical Information, Model Number US18650H2, Li-ion Division, RME Company Sony Corporation, 1998.
- [14] G. Ning, et al., Capacity fade study of lithium-ion batteries cycled at high discharge rates, J. Power Sources 117 (2003) 160–169.
- [15] L.P. Jarvis, et al., Fuel cell/electrochemical capacitor hybrid for intermittent high power applications, J. Power Sources 79 (1999) 60–63.